Neurochemistry International 100 (2016) 67–77

Contents lists available at ScienceDirect

Neurochemistry International

journal homepage: www.elsevier.com/locate/nci

Bupropion and its photoreactive analog (±)-SADU-3-72 interact with luminal and non-luminal sites at human α4β2 nicotinic acetylcholine receptors

Hugo R. Arias [a, *], Dominik Feuerbach [b], Marcelo O. Ortells [c]

[a] Department of Medical Education, California Northstate University College of Medicine, Elk Grove, CA, USA
[b] Novartis Institutes for Biomedical Research, Basel, Switzerland
[c] Facultad de Medicina, Universidad de Morón, Morón, CONICET, Argentina

ARTICLE INFO

Article history:
Received 3 May 2016
Received in revised form
5 August 2016
Accepted 31 August 2016
Available online 6 September 2016

Keywords:
Human α4β2 nicotinic acetylcholine receptor
Bupropion
(±)-SADU-3-72
Molecular docking
Luminal and non-luminal sites
Ca^{2+} influx

ABSTRACT

The interaction of (±)-bupropion [(±)-BP] with the human (h) α4β2 nicotinic acetylcholine receptor (AChR) was compared to that for its photoreactive analog (±)-2-(*N*-*tert*-butylamino)-3′-iodo-4′-azidopropiophenone [(±)-SADU-3-72]. Ca^{2+} influx results indicated that (±)-SADU-3-72 and (±)-BP inhibit hα4β2 AChRs with practically the same potency. However, (±)-SADU-3-72 binds to the [^{3}H]imipramine sites at resting and desensitized hα4β2 AChRs with 3-fold higher affinity compared to that for (±)-BP, which is supported by molecular docking results. The docking results also indicate that each isomer of BP and SADU-3-72, in the protonated state, interacts with luminal and non-luminal sites. In the channel lumen, both ligands bind to two overlapping subsites, one that overlaps the imipramine site, and another much closer to the cytoplasmic side. The results suggest, for the first time, three differentiated non-luminal domains, including the transmembrane (TMD), extracellular (ECD), and ECD-TMD junction. In the ECD-TMD junction, BP and SADU-3-72 bind to overlapping sites. Interestingly, only SADU-3-72 binds to intrasubunit and intersubunit sites in the TMD, and to additional sites in the ECD. Our results are consistent with a model where BP and SADU-3-72 bind to overlapping sites in the luminal and ECD-TMD junctional domains of the hα4β2, whereas only SADU-3-72 binds to additional non-luminal sites. The BP junctional site opens the door for additional inhibitory mechanisms. The pharmacological properties of (±)-SADU-3-72 showed in this work support further photolabeling studies to mapping the BP binding sites in the hα4β2 AChR.

1. Introduction

(±)-Bupropion [(±)-BP; (±)-2-(*tert*-butylamino)-1-(3-chlorophenyl)propan-1-one] (see the molecular structures of the (*S*)-(+)- and (*R*)-(−)-enantiomers in Fig. 1) was originally developed as an antidepressant (Wellbutrin®) but is also currently used as a smoking cessation aid (Zyban®) (reviewed in (Arias, 2009; Arias et al., 2014)). It is believed that the antidepressant activity of (±)-BP is due to its inhibitory action on the dopamine and norepinephrine reuptake systems. However, new evidence suggests that the antidepressant and anti-addictive properties of (±)-BP are also due to the noncompetitive antagonistic activity on several nicotinic acetylcholine receptors (AChRs) (reviewed in (Arias, 2009; Arias et al., 2014)). AChRs are members of the Cys-loop ligand-gated ion channel superfamily that include type A and C γ-aminobutyric acid, type 3 5-hydroxytryptamine (serotonin) (i.e., 5-HT_3R), and glycine receptors (reviewed in (Arias, 2006; Kamens et al., 2011)).

The structural characterization of the BP binding sites in neuronal AChRs is relevant for the development of novel BP

Abbreviations: AChR, nicotinic acetylcholine receptor; NCA, noncompetitive antagonist; (±)-BP, (±)-bupropion [(±)-2-(*tert*-butylamino)-1-(3-chlorophenyl) propan-1-one]; (±)-SADU-3-72, (±)-2-(*N*-*tert*-butylamino)-3′-iodo-4′-azidopropiophenone; ECD, extracellular domain; TMD, transmembrane domain; H-bond, hydrogen bond; MD, molecular dynamics; RMSD, root mean square deviation; AVG, average RMSD value; VAR, RMSD variance; κ-BTx, κ-bungarotoxin; RT, room temperature; BS, binding saline; K_i, inhibition constant; K_d, dissociation constant; IC_{50}, ligand concentration that inhibits 50% binding or Ca^{2+} influx; n_H, Hill coefficient; DMEM, Dulbecco's Modified Eagle Medium; FBS, fetal bovine serum.

* Corresponding author. Department of Medical Education, California Northstate University College of Medicine, 9700 W. Taron Dr., Elk Grove, CA 95757, USA.
E-mail address: hugo.arias@cnsu.edu (H.R. Arias).

http://dx.doi.org/10.1016/j.neuint.2016.08.013
0197-0186/

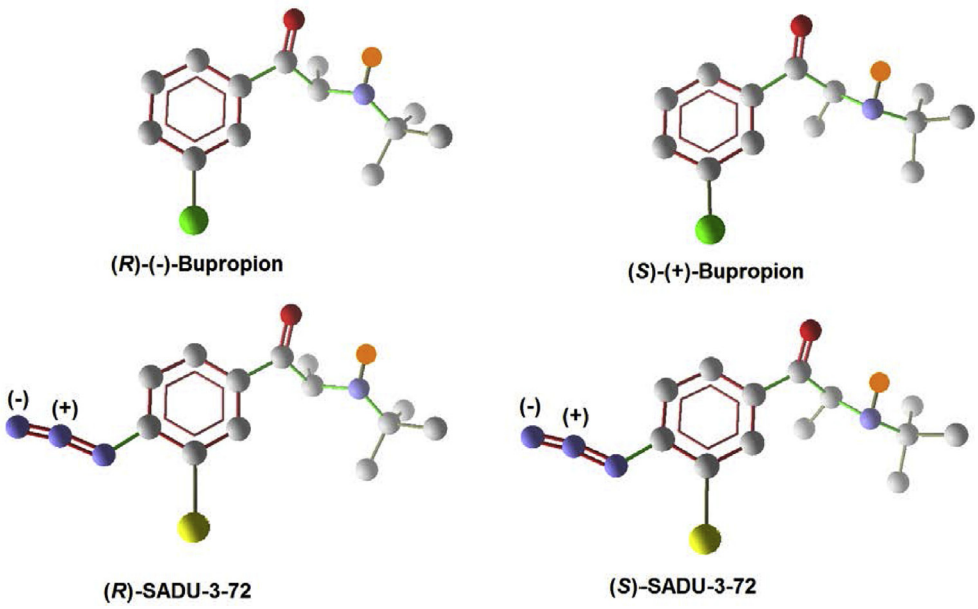

Fig. 1. Molecular structure of (*S*)-(+)- and (*R*)-(−)-bupropion [(*S*)-(+)- and (*R*)-(−)-2-(*tert*-butylamino)-1-(3-chlorophenyl)propan-1-one], and its photoreactive analogs (*S*)- and (*R*)-SADU-3-72 [(*S*)- and (*R*)-2-(*N-tert*-butylamino)-3'-iodo-4'-azidopropiophenone]. The chloride atom is rendered in green, iodine in yellow, carbon in gray, nitrogen in blue, oxygen in red, and hydrogen in orange. In SADU-3-72, the iodine atom (yellow) and the photoreactive azide group (blue), possessing negative and positive charges, are located at positions 3′ and 4′, respectively, on the aromatic ring. The ligands are shown in the ball and stick mode. (For interpretation of the references to colour in this figure legend, the reader is referred to the web version of this article.)

derivatives with improved clinical profiles for treating depression, nicotine addiction, and psychostimulant abuse. In this regard, a photoreactive analog of (±)-BP, (±)-2-(*N-tert*-butylamino)-3'-iodo-4'-azidopropiophenone [(±)-SADU-3-72] (see molecular structures of the (*S*)- and (*R*)-enantiomers in Fig. 1), has been developed for photoaffinity labeling studies (Lapinsky et al., 2012). The pharmacological and structural features of (±)-SADU-3-72 (Arias et al., 2012) and the photolabeling of the BP binding sites in the resting and desensitized states were recently studied in muscle AChRs (Pandhare et al., 2012). Following the characterization of BP interacting with neuronal AChRs, which is more clinically relevant, we determined, in this work, the pharmacological properties of (±)-SADU-3-72 at the α4β2 AChR, the most abundant AChR in the brain, with the purpose of laying the basis for further photoaffinity labeling studies. In this regard, the functional and structural properties of BP interacting with this AChR subtype are compared to that for SADU-3-72 by means of Ca^{2+} influx, [^{3}H]imipramine binding, and molecular modeling studies. For the molecular modeling studies, we took advantage of the new crystallographic structure of the homopentameric mouse (m) 5-HT_{3A}R at 3.5 Å resolution (PDB ID: 4PIR) (Hassaine et al., 2014) to build the human (h) α4β2 AChR by homology modeling. Considering that the interaction of imipramine with hα4β2 AChRs has been previously characterized (Arias et al., 2010a), [^{3}H]imipramine competition binding assays are performed to determine the interaction of (±)-BP and (±)-SADU-3-72 with these binding sites. The results from the present work give information about the interaction of BP with hα4β2 AChRs in different conformational states, and will pave the way for further photolabeling studies using (±)-SADU-3-72 as a probe for the BP sites at the α4β2 AChR.

2. Methods and materials

2.1. Ca^{2+} influx measurements in the HEK293-hα4β2 cell line

The HEK293-hα4β2 cell line was cultured as described previously (Arias et al., 2010a, 2013a,b, 2015). Under these conditions, the AChRs are predominantly expressed with the $(\alpha4)_3(\beta2)_2$ stoichiometry (Arias et al., 2013b). Ca^{2+} influx experiments were performed as previously described (Arias et al., 2010a, 2013a,b, 2015). Briefly, 5×10^4 cells per well were seeded 48 h prior to the Ca^{2+} influx experiment on black poly-L-lysine 96-well plates (Costar, Corning Inc., New York, USA) and incubated at 37 °C in a humidified atmosphere (5% CO_2/95% air). 16 h before the experiment, the medium was changed to 1% bovine serum albumin (BSA) in HEPES-buffered salt solution (HBSS) (130 mM NaCl, 5.4 mM KCl, 2 mM $CaCl_2$, 0.8 mM $MgSO_4$, 0.9 mM NaH_2PO_4, 25 mM glucose, 20 mM HEPES, pH 7.4). On the day of the experiment, the medium was removed by flicking the plates and replaced with 100 μL HBSS/1% BSA containing 2 μM Fluo-4 (Molecular Probes, Eugene, OR, USA) in the presence of 2.5 mM probenecid (Sigma, Buchs, Switzerland). The cells were then incubated at 37 °C in a humidified atmosphere (5% CO_2/95% air) for 1 h. Plates were flicked to remove excess of Fluo-4, washed twice with HBSS/1% BSA, and finally refilled with 100 μL of HBSS containing different concentrations of BP or (±)-SADU-3-72, and pre-incubated for 5 min. Plates were then placed in the cell plate stage of the fluorimetric imaging plate reader (Molecular Devices, Sunnyvale, CA, USA). A baseline consisting of 5 measurements of 0.4 s each was recorded. (±)-Epibatidine (0.1 μM) was then added from the agonist plate to the cell plate using the 96-tip pipettor simultaneously to fluorescence recordings for a total length of 3 min. The laser excitation and emission wavelengths were 488 and 510 nm, at 1 W, with a CCD camera opening of 0.4 s.

2.2. [^{3}H]Imipramine binding experiments using hα4β2 AChRs in different conformational states

The effect of (±)-BP and (±)-SADU-3-72 on [^{3}H]imipramine binding to hα4β2 AChRs in different conformational states was studied as described previously (Arias et al., 2010a, 2013a,b). In this regard, hα4β2 nAChR membranes (1.5 mg/mL) were suspended in

binding saline buffer (50 mM Tris-HCl, 120 mM NaCl, 5 mM KCl, 2 mM $CaCl_2$, 1 mM $MgCl_2$, pH 7.4) with 15 nM [^{3}H]imipramine in the presence of 0.5 μM (±)-epibatidine (desensitized/agonist-bound state) or 0.1 μM κ-BTx (resting/κ-BTx-bound state), and preincubated for 30 min at RT. κ-BTx is a high-affinity competitive antagonist that maintains the AChR in the resting (closed) state (Moore and McCarthy, 1995). Nonspecific binding was determined in the presence of 100 μM imipramine.

The total volume was divided into aliquots, and increasing concentrations of the ligand under study were added to each tube and incubated for 2 h at RT. AChR-bound radioligand was then separated from free ligand by a filtration assay using a 48-sample harvester system with GF/B Whatman filters (Brandel Inc., Gaithersburg, MD, USA), previously soaked with 0.5% polyethylenimine for 30 min. The membrane-containing filters were transferred to scintillation vials with 3 mL of Bio-Safe II (Research Product International Corp, Mount Prospect, IL, USA), and the radioactivity was determined using a Beckman LS6500 scintillation counter (Beckman Coulter, Inc., Fullerton, CA, USA).

The concentration–response data were curve-fitted by nonlinear least squares analysis using the Prism software. The corresponding IC_{50} values were transformed into inhibition constant (K_i) values using the Cheng–Prusoff relationship (Cheng and Prusoff, 1973):

$$K_i = IC_{50} \Big/ \left\{ 1 + \left([[^3\text{H}]\text{imipramine}] \Big/ K_d^{\text{imipramine}} \right) \right\} \quad (1)$$

where [[^{3}H]imipramine] is the initial concentration of [^{3}H]imipramine, and $K_d^{\text{imipramine}}$ corresponds to the dissociation constant of [^{3}H]imipramine for the hα4β2 AChR (0.83 μM) (Arias et al., 2010a). The calculated K_i and n_H values are summarized in Table 2.

2.3. Molecular docking and molecular dynamics of BP and SADU-3-72 isomers in hα4β2 AChRs

The hα4β2 nAChR was built by homology modeling using the X-ray structure (PDB ID: 4PIR; 3.5 Å resolution) of the homopentameric m5-HT_{3A}R (Hassaine et al., 2014) as the template, and employing the programs Modeller 9.8 (Šali and Blundell, 1993) and SWIFT MODELLER (Mathur and Shankaracharya Vidyarthi, 2011). For this purpose, the amino acid sequences of the hα4 and hβ2 subunits were first aligned with the sequence of the m5-HT_{3A} subunit by using the ClustalW2 server (www.ebi.ac.uk/Tools/msa/clustalw2) (Thompson et al., 1994). The resulting hα4β2 nAChR structure was energy minimized using molecular mechanics with the program NAMD (Phillips et al., 2005), CHARMM force field (Brooks et al., 1983), and the software VEGA ZZ (version 3.0.5.12) as interface (Pedretti et al., 2004). The energy minimization was carried out fixing the backbone atoms to their original positions, to avoid distorting the secondary structure. To evaluate the model accuracy, the Modeller DOPE score (Šali and Blundell, 1993) was calculated and compared to the value obtained with the original m5-HT_{3A}R X-ray structure (Hassaine et al., 2014).

Each R- and S-isomer of BP and SADU-3-72, in the protonated state, were first modeled using VEGA ZZ. Minimization and partial charge calculations were done using the MOPAC program as implemented in VEGA ZZ and employing the semiempirical AM1 method. Subsequently, each molecule was docked into the whole hα4β2 AChR model using AutoDock Vina (Trott and Olson, 2010). The parameters used with AutoDock Vina, were exhaustiveness = 570 (the maximum value allowed by our computational system), and maximum number of modes = 20. To achieve dockings in few minutes time regime, no flexible residues were allowed in the receptor models. The program gives clusters of superposed conformations from the 20 highest binding affinity poses.

To test the stability of each BP and SADU-3-72 poses within their predicted docking sites, 20-ns MD simulations were performed using NAMD and CHARMM force field, and VEGA ZZ as interface. To estimate the ligand binding energies, the Adaptive Poisson-Boltzmann Solver (ABPS) implementation within Vega ZZ (Baker et al., 2001) was used. Theoretical binding energies were measured from the individual poses at 15 and 20 ns. The poses with a maximum binding energy of −25 kJ/mol, corresponding to a K_i = 34 μM (Tables S1–S4; Supplemental Material), an affinity closer to the experimental value, were used in this work.

The hα4β2 nAChR model was first hydrated with a 10 Å minimum thick shell using the program solvate 1.0 (Grubmueller, 1996), which also added the appropriated number of Cl^- and Na^+ to neutralize the system, and the model subsequently minimized using NAMD. The MD protocol includes a timestep size of 1 fs, with 20 timesteps per cycle (the number of timesteps between atom reassignments). The cutoff value for non-bond energy evaluation was 12 Å. A distance of 8 Å for the switching function was used. Pairs of bonded atoms excluded from non-bonded interaction calculations was determined to 1–4, that is, no non-bonded interactions were calculated for lists of 4 consecutive bonded atoms. The MD simulations were performed in three stages: (1) the system was heated from 0 to 300 K, increasing the temperature 25 K for every 500 fs (6 ps), (2) a system equilibration was performed during 200 ps followed by the 20-ns production simulation, and (3) the temperature of the system was rescaled every 1000 steps to 300 K. During the MD simulation, and to reduce computation time, all residues and water molecules outside a 20 Å radius sphere and centered on the corresponding ligand pose were restricted to their original positions whilst those within this sphere were free to move. The same size sphere was used to implement a spherical periodic boundary condition (Lewards, 2011). To estimate the root mean square deviation (RMSD) values with respect to the initial structure (see (Arias et al., 2013b)), the conformations during the simulation were extracted every 10-ps from the simulation trajectory of 20-ns total time by using VEGA ZZ.

$$\text{RMSD} = \sqrt{\frac{\sum_{i=1}^{N} \partial_i^2}{N}} \quad (2)$$

where, N is the number of atoms from the ligand, and is the distance between the corresponding ligand atoms obtained at each step and the starting conformation. The average (AVG) RMSD values are a reference of the movement of the ligand from its original docking site. Large AVG values do not only mean that the ligand moves away from the original site, but mostly implies more rotations within the site. The poses with a variance (VAR) RMSD value below 0.5 during the last 5-ns of the MD where used in this work (Tables S1–S4; Supplemental Material).

2.4. Materials

[^{3}H]Imipramine (47.5 Ci/mmol) was obtained from PerkinElmer Life Sciences Products, Inc. (Boston, MA, USA) and stored in ethanol at −20 °C. (±)-SADU-3-72 [(±)-2-(*N*-*tert*-butylamino)-3'-iodo-4'-azidopropiophenone] was synthesized as described in Lapinsky et al. (2012). Imipramine hydrochloride and polyethylenimine were purchased from Sigma-Aldrich Chemical Co. (St. Louis, MO, USA). (±)-Epibatidine hydrochloride was obtained from Tocris Bioscience (Ellisville, MO, USA). κ-Bungarotoxin (κ-BTx) was obtained from Biotoxins Incorporated (St. Cloud, FL, USA). (±)-Bupropion hydrochloride [(±)-BP] [(±)-2-(*tert*-butylamino)-1-

(3-chlorophenyl)propan-1-one] was obtained through the National Institute on Drug Abuse (NIDA) (NIH, Baltimore, MD, USA). Fetal bovine serum (FBS) and trypsin/EDTA were purchased form Gibco BRL (Paisley, UK). Salts were of analytical grade.

3. Results

3.1. Inhibition of (±)-epibatidine-mediated Ca^{2+} influx in hα4β2 AChRs by (±)-BP and (±)-SADU-3-72

The potency of (±)-epibatidine to activate hα4β2 AChRs was first determined by assessing the fluorescence change in HEK293-hα4β2 cells after (±)-epibatidine stimulation (Fig. 2A). The observed EC_{50} value (30 ± 5 nM) is in the same concentration range as those previously determined (Arias et al., 2010a, 2013a, 2013b, 2015). Pre-incubation with (±)-BP or (±)-SADU-3-72 subsequently blocked the observed (±)-epibatidine-induced AChR activation (Fig. 2A,B). Comparing the calculated IC_{50} values, no statistical difference between (±)-BP and (±)-SADU-3-72 in inhibiting hα4β2 AChRs was found ($p > 0.05$) (Table 1). Although the n_H values for (±)-BP and (±)-SADU-3-72 are not statistically different from each other ($p = 0.37$), the value for (±)-BP is closer to unity, suggesting a noncooperative mechanism for this ligand. A similar n_H value was previously obtained for (±)-SADU-3-72-induced inhibition of human muscle AChRs (Arias et al., 2012).

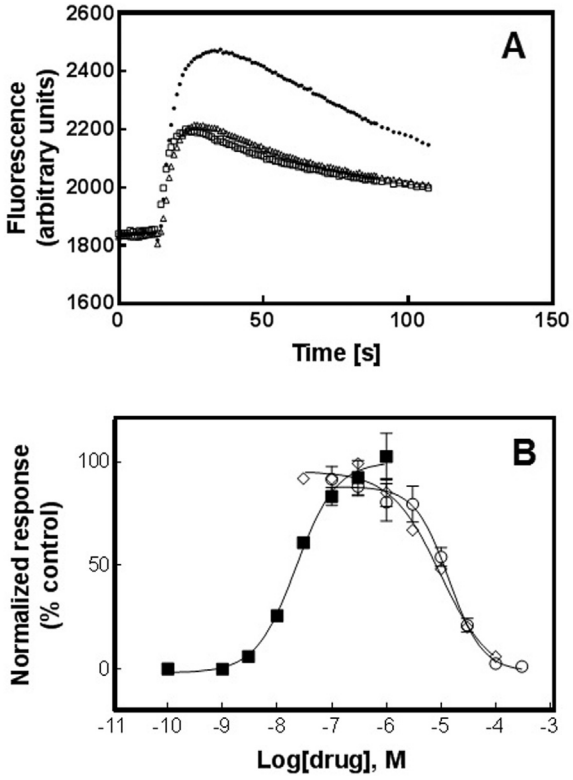

Fig. 2. Inhibitory effect of (±)-bupropion and (±)-SADU-3-72 on (±)-epibatidine-induced Ca^{2+} influx in HEK293-hα4β2 cells. (A) (±)-Bupropion (Δ) and (±)-SADU-3-72 (□) (10 μM each) decreased Ca^{2+} influx-induced fluorescence produced by 0.1 μM (±)-epibatidine (●). (B) Increased concentrations of (±)-epibatidine (■) activate hα4β2 AChRs with potency $EC_{50} = 30 \pm 5$ nM ($n = 28$). Subsequently, cells were pre-treated with several concentrations of (±)-bupropion (○) or (±)-SADU-3-72 (◊), followed by addition of 0.1 μM (±)-epibatidine. Response was normalized to the maximal (±)-epibatidine response which was set as 100%. The plots are the average of seven (○) and five (◊) separate determinations, respectively, where the error bars correspond to the S.D. The calculated IC_{50} and n_H values are summarized in Table 1.

Table 1
Inhibitory potency of (±)-bupropion and (±)-SADU-3-72 for the hα4β2 AChR determined by Ca^{2+} influx assays.

Ligand	IC_{50} (μM)[a]	n_H[b]
(±)-Bupropion	17.8 ± 2.2	1.17 ± 0.12
(±)-SADU-3-72	15.2 ± 2.1	1.31 ± 0.06

[a] The values for (±)-bupropion and (±)-SADU-3-72 were obtained from Fig. 2.
[b] Hill coefficient.

3.2. Inhibition of [^{3}H]imipramine binding to hα4β2 AChRs in different conformational states elicited by (±)-BP and (±)-SADU-3-72

The binding affinity of (±)-BP and (±)-SADU-3-72 for hα4β2 AChRs in different conformational states was studied by [^{3}H]imipramine competition binding experiments. (±)-BP (Fig. 3A) and (±)-SADU-3-72 (Fig. 3B) inhibit the specific binding of [^{3}H]imipramine in a concentration-dependent fashion in either the desensitized or resting state. The binding affinity for (±)-SADU-3-72 is 3-fold higher ($p < 0.05$) than that for (±)-BP in either the resting or desensitized state (Table 2). (±)-BP and (±)-SADU-3-72 do not discriminate between the resting and desensitized states, which is in agreement to that observed for (±)-SADU-3-72, but not for (±)-BP, in the *Torpedo* AChR (Arias et al., 2012). The calculated n_H values for (±)-BP and (±)-SADU-3-72 are close to unity (Table 2), indicating that these ligands inhibit [^{3}H]imipramine binding in a noncooperative manner. These results also suggest that (±)-BP and (±)-SADU-3-72 overlap the [^{3}H]imipramine binding sites.

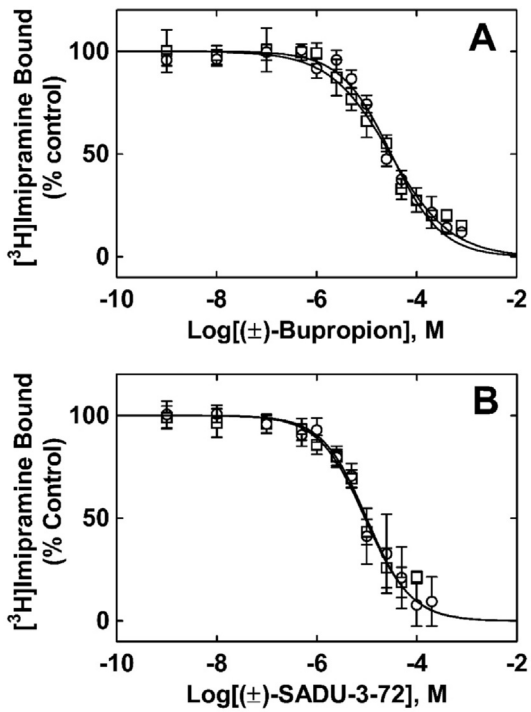

Fig. 3. Inhibition of [^{3}H]imipramine binding to hα4β2 AChRs by (A) (±)-bupropion and (B) (±)-SADU-3-72, respectively. hα4β2 AChR membranes (1.5 mg/mL) were equilibrated (2 h) with 15 nM [^{3}H]imipramine, in the presence of 0.1 μM κ-BTx (resting/κ-BTx-bound) (○) or 0.5 μM (±)-epibatidine (□) (desensitized/epibatidine-bound state), and increasing concentrations of the ligand under study. Nonspecific binding was determined at 100 μM imipramine. Each plot is the combination of 2–4 separate experiments, where the error bars correspond to the S.D. The IC_{50} and n_H values were obtained by nonlinear least-squares fit, and subsequently, the K_i values were calculated using Eq. (1) and summarized in Table 2.

Table 2
Binding affinity of (±)-bupropion and (±)-SADU-3-72 for the [^{C}H]imipramine binding sites at hα4β2 AChRs in different conformational states.

Ligand	Conformational state	K_i[a] (μM)	n_H[b]	(±)-Bupropion/ (±)-SADU-3-72 ratio
(±)-Bupropion	Resting/κ-BTx-bound	30.5 ± 3.1	0.95 ± 0.08	3.1
	Desensitized/Epibatidine-bound	29.3 ± 4.2	0.71 ± 0.07	3.2
(±)-SADU-3-72	Resting/κ-BTx-bound	9.8 ± 1.6	0.97 ± 0.13	–
	Desensitized/Epibatidine-bound	9.1 ± 1.1	0.94 ± 0.11	–

[a] The K_i values were obtained from Fig. 3A,B, respectively, according to Eq. (1).
[b] Hill coefficient.

3.3. *Molecular docking and molecular dynamics simulations of BP and SADU-3-72 isomers in hα4β2 AChRs*

The Modeller DOPE values for the original m5-HT_{3A}R X-ray structure (Hassaine et al., 2014) and the built hα4β2 AChR model were very similar (−251378.33 and −251378.48, respectively), supporting the structural quality of the used hα4β2 AChR model.

According to the molecular docking results, both (R)- and (S)-isomers of BP and SADU-3-72, in the protonated state, bind to luminal and non-luminal sites. Initially, twelve and thirteen different poses were observed for (R)- and (S)-BP, respectively, as well as eighteen and sixteen poses for (R)- and (S)-SADU-3-72, respectively (Tables S1–S4; Supplemental Material). To evaluate the stability of the different poses, 20-ns MD simulations were performed, and the RMSD values during the last 5-ns of the simulation calculated.

Four main domains where found within the hα4β2 nAChR where these molecules bind: a luminal domain with two overlapping subsites, as well as three different non-luminal domains (Fig. 4; Tables 3 and S1), the ECD-TMD junction (Fig. 5; Tables 4 and S2), the transmembrane domain (TMD), where both intrasubunit and intersubunit sites are located (Fig. 6; Tables 5 and S3), and the extracellular domain (ECD) with additional sites (i.e., vestibular and interfacial) located in the vestibule (Table S4; Fig. S1; Supplemental Material).

In the luminal domain, two overlapping subsites were observed (Fig. 4; Table 3): a subsite (i.e., L subsite), with one pose for each isomer (R)-BP, (R)-SADU-3-72, and (S)-SADU-3-72, starting at position 13' (valine ring) and extending to position -3′, near the cytoplasmic M1-M2 loop, and the cytoplasmic (Cyt) subsite, with three poses for each (R)-BP and (S)-SADU-3-72, one for (S)-BP, and two for (R)-SADU-3-72, located much closer to the cytoplasmic end, between positions -2′ (intermediate ring) and -5′ (cytoplasmic or inner ring). In the L subsite, a stable hydrogen bond (H-bond) interaction between either (R)-BP (pose 1) or (R)-SADU-3-72 (pose 1) and β2-E239 (position -2′) was found (Table 7). (R)-SADU-3-72 (pose 1) also maintains a relatively stable H-bond with β2-T242 (position 2′), whereas the (S)-isomer (pose 1) forms a stable H-bond and salt bridge with α4-E266 at the M2 extracellular end. In addition, (R)-BP (pose 1) forms a salt bridge with β2-E239, whereas (R)-SADU-3-72 (pose 1) forms two salt bridges with the same residue from two β2 subunits (Table 7). In the Cyt subsite, all BP poses make stable H-bonds with β2-E239 (position -2′). (R)-SADU-3-72 (pose 1) makes stable H-bonds with β2-E239 and α4-E245 (position -2′), whereas (R)-SADU-3-72 (pose 2) makes significant H-bond only with the former. All (R)-BP poses make salt bridges with two E239 residues, one from each β2 subunit, whereas (S)-BP makes salt bridges with both β2-E239 and α4-E245. The same interactions with β2-E239 and α4-E245 are observed with all poses of (R)- and (S)-SADU-3-72, except pose 3 of the latter which only forms a salt bridge with α4-E245.

In the ECD-TMD junction, three different sites were found at the respective +α4/-β2, -β2/+α4, and +β2/-β2 interfaces (Fig. 5;

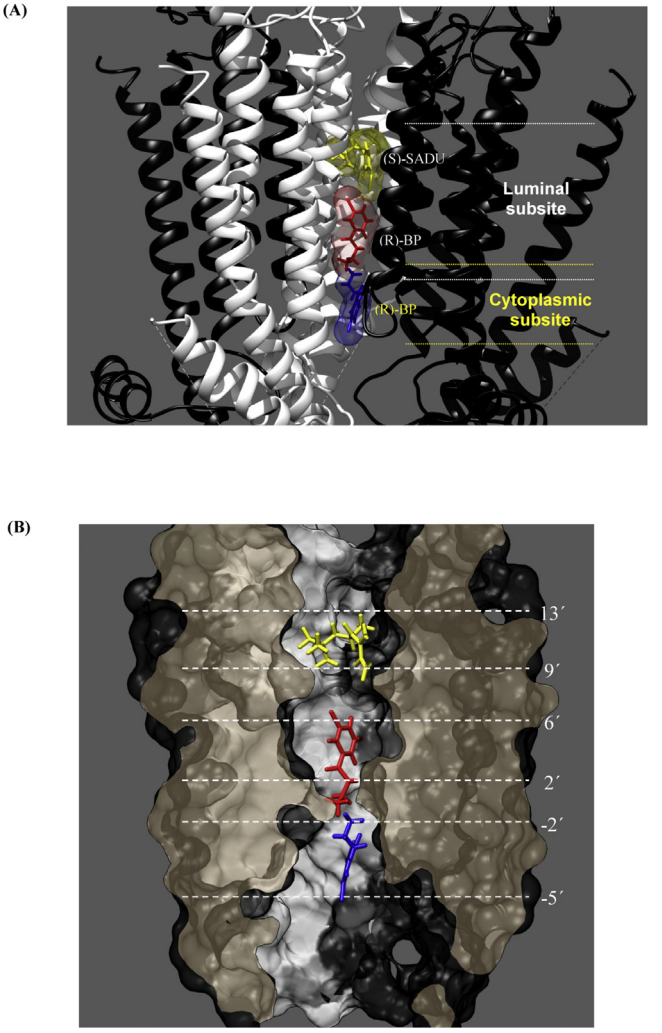

Fig. 4. Molecular docking of BP and SADU-3-72 isomers to the hα4β2 AChR ion channel. **(A)** Two overlapping subsites were observed in the ion channel: a luminal (L) subsite with one pose for (R)-BP, (R)-SADU-3-72, and (S)-SADU-3-72, and a cytoplasmic (Cyt) subsite, with three poses for each (R)-BP and (S)-SADU-3-72, one for (S)-BP, and two for (R)-SADU-3-72. For simplicity, only (R)-BP (pose 1; red) and (S)-SADU-3-72 (pose 1; yellow) are shown in the L subsite, and (R)-BP (pose 4; blue) in the Cyt subsite. The receptor is shown as ribbons, while the ligands are shown as sticks with their solvent accessible surface around them. **(B)** The L subsite is located at position 13′ (valine ring) and extends to position -3′, whereas the Cyt subsite is located much closer to the cytoplasmic end, including positions -2′ (intermediate ring) and -5′ (cytoplasmic or inner ring). The M2 rings at position 13′, 9′, 6′, 2′, -2′, and -5′ are also marked. The receptor is depicted by its solvent accessible surface, while the ligands are shown as sticks. The α4 and β2 subunits are depicted in white and black, respectively. See Tables 3 and 7 for details on the involved residues. (For interpretation of the references to colour in this figure legend, the reader is referred to the web version of this article.)

Table 3
Molecular docking of bupropion and SADU-3-72 isomers to the hα4β2 nAChR ion channel, including the luminal (L) and cytoplasmic (Cyt) subsites.

Subsite	Isomer (Pose)	M2 (Position)		M1-M2 Loop (Position)		
L	(R)-BP	α4-L249 (3′)	β2-L249 (9′)	α4-E245 (−2′)	**β2-E239 (-2′)**	
	(1)	α4-T248 (2′)	β2-S246 (6′)			
			β2-I245 (5′)			
			β2-T242 (2′)			
	(R)-SADU-3-72	α4-L255 (9′)	β2-L249 (9′)	α4-E245 (−2′)	**β2-E239 (-2′)**	
	(1)	α4-S252 (6′)	β2-S246 (6′)	α4-G244 (−3′)	β2-G238 (−3′)	
		α4-I251 (5′)	β2-I245 (5′)			
		α4-T248 (2′)	β2-L243 (3′)			
		α4-I247 (1′)	**β2-T242 (2′)**			
			β2-M241 (1′)			
	(S)-SADU-3-72	**α4-E266 (20′)**				
	(1)	α4-V259 (13′)	β2-V253 (13′)			
		α4-T258 (12)'	β2-A250 (10′)			
		α4-S256 (10′)	β2-L249 (9′)			
		α4-L255 (9′)	β2-V247 (7′)			
		α4-S252 (6′)	β2-S246 (6′)			
Cyt	(R)-BP	α4-S252 (6′)	β2-S246 (6′)		β2-K240 (−1′)	
	(1)	α4−I251 (5′)	β2-I245 (5′)		**β2-E239 (-2′)**	
		α4-T248 (2′)	β2-T242 (2′)			
	(R)-BP	α4-T248 (2′)	β2-T242 (2′)	α4-E245 (−2′)	**β2-E239 (-2′)**	β2-C237 (−4′)
	(2)		β2-M241 (1′)	α4-G244 (−3′)	β2-G238 (−3′)	
	(R)-BP	α4-S252 (6′)	β2-S246 (6′)	**β2-E239 (-2′)**		
	(3)	α4-I251 (5′)	β2-I245 (5′)	β2-G238 (−3′)		
		α4-T248 (2′)	β2-L243 (3′)			
			β2-T242 (2′)			
	(S)-BP	α4-T248 (2′)	β2-T242 (2′)	**α4-E245 (-2′)**	**β2-E239 (-2′)**	β2-C237 (−4)'
	(1)	α4-I247 (1′)	β2-M241 (1′)	α4-G244 (−3′)	β2-G238 (−3′)	
	(R)-SADU-3-72	α4-T248 (2′)	β2-T242 (2′)	**α4-E245 (-2′)**	**β2-E239 (-2′)**	β2-D236 (−5′)
	(1)		β2-M241 (1′)	α4-G244 (−3′)	β2-G238 (−3′)	
				α4-C243 (−4′)	β2-C237 (−4′)	
	(R)-SADU-3-72	α4-T248 (2′)	β2-T242 (2′)	**α4-E245 (-2′)**	**β2-E239 (-2′)**	
	(2)	α4-I247 (1′)	β2-M241 (1′)	α4-G244 (−3′)	β2-G238 (−3′)	
				α4-C243 (−4′)	β2-C237 (−4′)	
	(S)-SADU-3-72	α4-I251 (5′)	β2-S246 (6′)	α4-K246 (−1′)	α4-C243 (−4′)	**β2-E239 (-2′)**
	(1)	α4-T248 (2′)	β2-M241 (1′)	**α4-E245 (-2′)**	α4-E242 (−5′)	β2-G238 (−3′)
		α4-I247 (1′)		α4-G244 (−3′)		β2-C237 (−4′)
	(S)-SADU-3-72	α4-T248 (2′)		**α4-E245 (-2′)**	**β2-E239 (-2′)**	β2-D236 (−5′)
	(2)			α4-G244 (−3′)	β2-G238 (−3′)	
				α4-C243 (−4′)	β2-C237 (−4′)	
	(S)-SADU-3-72	α4-T248 (2′)		α4-E245 (−2′)	β2-K240 (−1′)	β2-C237 (−4′)
	(3)	α4-I247 (1′)	β2-M241 (1′)	α4-G244 (−3′)	**β2-E239 (-2′)**	β2-D236 (−5′)
				α4-C243 (−4′)	β2-G238 (−3′)	

Residues in bold indicate hydrogen bond and/or a salt bridge formation (see Table 7 for more details).

Table 4). In the +α4/-β2 interface, (R)-BP (pose 1) and (R)-SADU-3-72 (pose 2) bind to equivalent but not overlapping sites. In the ECD portion, (R)-BP interacts with α4 residues located in the β1-β2 loop, extracellular ion channel's mouth, and M2-M3 loop. (R)-BP establishes H-bonds with α4-D47 and α4-E266 but only a salt bridge with α4-D47, and makes contact with β2 residues, including G176 and E177 (i.e., β8-β9 loop) and R207 (i.e., end of the β10 β-strand). (R)-SADU-3-72 forms stable H-bonds with α4-E50 (β1-β2 loop) and α4-D143 (Cys-loop), and a salt bridge with the former residue, and interacts with residues from the M2-M3 loop and from the extracellular mouth. (R)-SADU-3-72 also make contacts with one α4-M1 and three β2-M1 residues, where β2-I214 and β2-N215 are shared with (R)-BP, as well as with additional α4-M3 residues not observed in the interaction with (R)-BP. (R)-BP interacts with β2-M1 residues, and with α4-E266 (20′) and α4-T265 (19′), forming a H-bond with the former. However, the side chain of α4-E266 points opposite to (R)-SADU-3-72. In the -β2/+α4 interface, only (R)-SADU-3-72 (pose 1) was found interacting with residues from the extracellular mouth, β2 residues from the M2-M3 loop and β1-β2 loop, α4-M1 residues, and three M2 residues from each subunit. Interestingly, (R)-SADU-3-72 forms stable H-bonds and salt bridges with both α4-D47 and α4-E50. Only (S)-SADU-7-32 (pose 1) was found in the +β2/-β2 interface, making contact only with β2 residues from the M2-M3 loop and M1-M3 segments. This isomer also forms stable H-bonds, but no salt bridges, with both β2-E47 (β1-β2 loop) and β2-D268 (M2-M3 loop).

In the TMD, two distinct non-luminal loci were observed only for the (S)-SADU-3-72 isomer (Fig. 6; Table 5): an intersubunit site, located closer to the extracellular side of the +α4/-β2 interface, and an intrasubunit site, located towards the cytoplasmic side of one β2-TMD. The intersubunit site comprises residues from one β2-M1 segment and from two adjacent α4-M2 and β2-M2 segments. Interestingly, (S)-SADU-3-72 makes a stable H-bond and a salt bridge with α4-E266 (position 20′), and a less stable H-bond with β2-D268. In the intrasubunit (β2) site, (S)-SADU-3-72 establishes a more stable H-bond with the M4-D434 side chain compared to that with the M1-F231 side chain. Although this isomer makes a salt bridge with D434, unlike previous conformers, it makes a second salt bridge with β2-D236.

In the ECD, three different sites for (R)- and (S)-SADU-3-72, but none for the BP isomers, were observed (Fig. S1; Table 6). The vestibular site is located in the extracellular vestibule, where (S)-SADU-3-72 (pose 1) binds to one of the β2 subunits mainly by van deer Waals contacts, and forms a H-bond and salt bridge with α4-D102. (R)-SADU-7-32 (pose 1) and (S)-SADU-7-32 (pose 2) interact with the +α4/-β2 interfacial site, which is facing the vestibule. (R)-SADU-3-72 establishes a stable H-bond and salt bridge with β2-E103, whereas (S)-SADU-3-72 makes stable H-bonds with the α4-

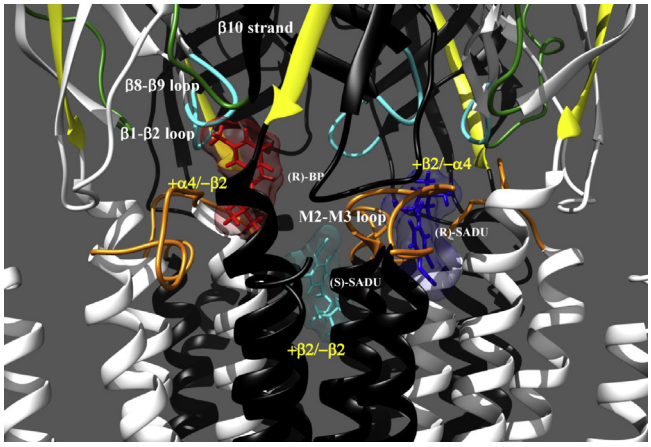

Fig. 5. Molecular docking of (R)-BP and SADU-3-72 isomers to the hα4β2 AChR extracellular-transmembrane (ECD-TMD) junction. (R)-BP (pose 1; red) interacts with the +α4/-β2 interface. (R)-SADU-3-72 (pose 2) also binds to the same site (not shown for simplicity). In addition, (R)-SADU-3-72 (pose 1; blue) interacts with the +β2/-α4 interface, whereas (S)-SADU-3-72 (pose 1; cyan) interacts with the +β2/-β2 interface. The most important structures in the ECD-TMD junction, including the M2-M3 loop, β1-β2 loop, β8-β9 loop, and β10 β-strand, are also shown. The α4 and β2 subunits are depicted in white and black, respectively. The receptor is shown as ribbons, while the ligands are shown as sticks with their solvent accessible surface around them. See Tables 4 and 7 for details on the involved residues. (For interpretation of the references to colour in this figure legend, the reader is referred to the web version of this article.)

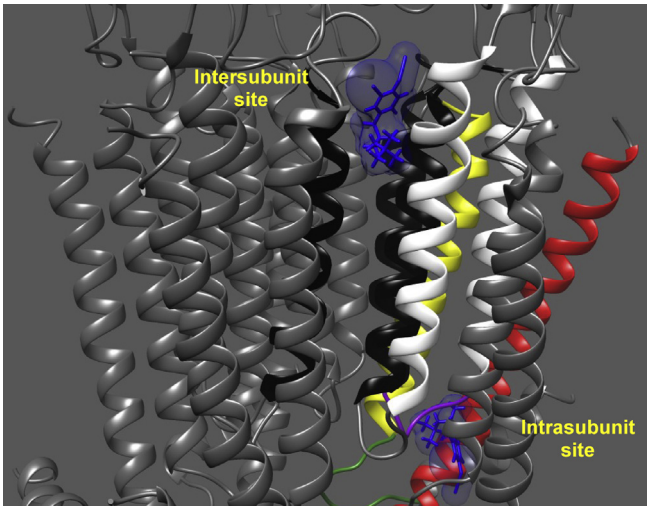

Fig. 6. Molecular docking of (S)-SADU-3-72 to the hα4β2 AChR transmembrane domain (TMD). Two non-overlapping sites for (S)-SADU-3-72 (ligand depicted as the solvent accessible surface) were observed: an intersubunit site located closer to the extracellular side of the +α4/-β2 interface, and an intrasubunit site located towards the cytoplasmic side of one β2-TMD. The intersubunit site comprises residues from one β2-M1 segment and two adjacent α4-M2 and β2-M2 segments. The receptor is depicted as ribbons in dark grey, whereas M1, M2, M3, M4, and M3-M4 loop are shown in black, white, yellow, red, and green, respectively. See Tables 5 and 7 for details on the involved residues. (For interpretation of the references to colour in this figure legend, the reader is referred to the web version of this article.)

D102 side chain and α4-I95 main chain, respectively, as well as a salt bridge with the former residue. In the -β2/+α4 interface, (R)-SADU-7-32 poses 2 and 3 make stable H-bonds with β2-D91 and β2-E103, and a salt bridge with β2-D91, whereas pose 2 forms an additional H-bond with β2-K85. The outer site is not included because it overlaps the orthosteric site and these compounds do not compete for the agonist sites (reviewed in (Arias, 2010)).

4. Discussion

The interaction of SADU-3-72 with hα4β2 AChRs was compared to that for BP, using functional and structural approaches, to determine whether (±)-SADU-3-72 can be used for further photolabeling studies on neuronal AChRs.

Our Ca^{2+} influx results indicate that both (±)-BP (17.8 ± 2.2 μM) and (±)-SADU-3-72 (15.2 ± 2.1 μM) inhibit hα4β2 AChRs with similar potency. By comparing these results with previous data, several conclusions can be made, including that (±)-SADU-3-72 inhibits hα1β1δε/γ AChRs (4.1 ± 0.7 and 1.4 ± 0.2, respectively) (Arias et al., 2012) with higher potency than that for hα4β2 AChRs.

Table 4
Molecular docking of bupropion and SADU-3-72 isomers to the extracellular-transmembrane (ECD-TMD) junction of the hα4β2 nAChR.

Subsite	Isomer (Pose)	ECD (Position)			M1	M2 (Position)		M3
+α4/-β2 Interface	(R)-BP	**α4-D47**	α4-S270	β2-G176	β2-F211	**α4-E266 (20′)**		
	(1)	α4-E50	α4-V274	β2-E177	β2-Y212	α4-T265 (19′)		
		α4-K51	α4-I275	β2-R207	β2-I214			
		α4-N52	α4-P269 (23′)		β2-N215			
			α4-I268 (22′)					
			α4-I267 (21′)					
	(R)-SADU-3-72	**α4-E50**	α4-S270		α4-L222	α4-T265 (19′)		α4-P276
	(2)	**α4-D143**	α4-V274		β2-I214	α4-I264 (18′)		α4-L277
			α4-P269 (23′)		β2-N215	α4-L261 (15′)		α4-I278
			α4-I268 (22′)		β2-I218			α4-G279
			α4-I267 (21′)					α4-E280
								α4-L282
								α4-L283
								α4-M286
+β2/−α4 Interface	(R)-SADU-3-72	**α4-D47**	β2-P264		α4-F217	α4-E266 (20′)	β2-K260 (20′)	
	(1)	**α4-E50**	β2-L267		α4-Y218	α4-I264 (18′)	β2-S259 (19′)	
		α4-I275	β2-V269		α4-I220	α4-F260 (14′)	β2-L256 (16′)	
		α4-I267 (21′)	β2-V269		α4-N221			
					α4-I224			
					α4-P225			
+β2/−β2 Interface	(S)-SADU-3-72	**β2-E47**			β2-I214	β2-L256 (16′)	β2-K260 (20′)	β2-M280
	(1)	β2-P264			β2-N215	β2-L255 (15′)	β2-S259 (19′)	
		β2-L267			β2-I218	β2-F254 (14′)	β2-I258 (18′)	
		β2-D268			β2-P219	β2-T252 (12′)	β2-L257 (17′)	
		β2-V269			β2-L222			

Residues in bold indicate hydrogen bond and/or a salt bridge formation (see Table 7 for more details).

Table 5
Molecular docking of (S)-SADU-3-72 to non-luminal sites located in the transmembrane domain of the hα4β2 nAChR.

Site (Pose)	M1	M2 (Position)		M2-M3 Loop (Position)	M3	M3-M4 Loop	M4
Intersubunit (1)	β2-Y212		β2-F254 (14′)	β2-I261 (21′)			
	β2-I214	α4-L261 (15′)		**β2-D268**			
	β2-N215	α4-L262 (16′)		α4-P269 (23′)			
	β2-L216	α4-L263 (17′)	β2-L257 (17′)				
	β2-I218		β2-I258 (18′)				
	β2-P219	α4-T265 (19′)					
		α4-E266 (20′)					
Intrasubunit (2)	**β2-F231**	β2-S235 (−6′)			β2-V293	β2-H297	β2-W426
	β2-L233	**β2-D236 (-5′)**			β2-L294	β2-H298	β2-K427
	β2-P234	β2-K240 (−1′)			β2-N295	β2-S300	β2-Y428
					β2-V296	β2-P301	β2-A430
						β2-T302	β2-M431
						β2-T303	**β2-D434**
							β2-R435

Residues until position 20′ are considered located in the ion channel, whereas residues beyond position 20′ are considered located in the M2-M3 loop.
Residues in bold indicate hydrogen bond and/or a salt bridge formation (see Table 7 for more details).

The observed inhibitory potency for (±)-BP is closer to that obtained for the $(\alpha4)_3(\beta2)_2$ stoichiometry (8.3 ± 1.2 μM) compared to that for the $(\alpha4)_2(\beta2)_3$ stoichiometry (46 ± 7 μM) (Papke et al., 2011), suggesting that our membrane preparation has higher density of $(\alpha4)_3(\beta2)_2$ AChRs, as previously considered (Arias et al., 2013b). Taking into account the results for (±)-BP at other human AChRs, the receptor selectivity follows the order: hα4β2 > hα1β1δε/γ (24.4 ± 3.3 and 23.4 ± 4.5, respectively) (Arias et al., 2009, 2012) ≫ hα7 (179 ± 20 μM) (Vázquez-Gómez et al., 2014). The observed IC_{50} value for (±)-BP is in the same concentration range as the calculated brain concentration (up to ~20 μM), when it is considered that BP can reach ~20-fold higher concentrations in the brain compared to that in plasma (~0.5–1 μM) (Hsyu et al., 1997).

The [^{3}H]imipramine competition results show additional pharmacological differences between (±)-BP and (±)-SADU-3-72. Although (±)-SADU-3-72 does not discriminate between the desensitized and resting hα4β2 AChRs, it presents 3-fold higher affinity than (±)-BP at either state, which is in agreement with the results obtained in *Torpedo* AChRs (Arias et al., 2012). In addition, (±)-BP does not discriminate between both hα4β2 AChR conformational states, contrary to the results obtained in *Torpedo* AChRs (Arias et al., 2009). Based on the observed noncooperative mechanism for the (±)-BP and (±)-SADU-3-72-induced inhibition of [^{3}H]imipramine binding (n_H ~1), these compounds may be interacting with the imipramine binding site in a steric fashion. In fact, docking results with hα4β2 AChRs indicate that the binding site for imipramine enantiomers, which is located between rings 9′ and 13′ (Arias et al., 2010a), partially overlaps the luminal subsite observed for BP and SADU-3-72, which is located between ring 13′ and position -3′. This location is in agreement with the photolabeling results using *Torpedo* AChRs showing that [^{125}I]-SADU-3-72 interacts with a domain formed between rings 2′ and 9′ (Pandhare et al., 2012). The wide binding domain determined by molecular docking includes the sites for other structurally different antidepressants such as fluoxetine (i.e., between rings 6′ and 13′) (Arias et al., 2010b), and (−)-reboxetine (i.e., between ring 6′ and position 14′)

Table 6
Molecular docking of SADU-3-72 isomers to sites located in the extracellular domain (ECD) of the hα4β2 nAChR.

Site	Subsite	Isomer (Pose)	ECD				
Vestibular	β2	(S)-SADU-3-72 (1)	β2-K19	β2-D91	β2-G100	β2-Y107	β2-P123
			β2-L58	β2-V92	β2-M101	β2-S108	β2-A124
			β2-Q60	β2-V93	β2-V104	β2-N109	β2-Y126
			β2-L89	β2-L94	β2-S105	β2-W120	β2-F148
			β2-P90	β2-N97	β2-F106	β2-P122	**α4-D102**
Interfacial	+α4/−β2	(R)-SADU-3-72 (1)	α4-K22	α4-E88	α4-P93	β2-R81	β2-H86
			α4-W23	α4-I90	α4-D94	β2-L82	**β2-E103**
			α4-S24	α4-W91	α4-D102	β2-P83	β2-F106
			α4-S87	α4-R92	α4-Y156	β2-S84	β2-S108
						β2-K85	β2-N109
		(S)-SADU-3-72 (2)	α4-K22	α4-E88	α4-D94	α4-Y156	β2-K85
			α4-W23	α4-I90	**α4-I95**	β2-R81	β2-S108
			α4-S24	α4-W91	α4-V96	β2-L82	β2-N109
			α4-Q63	α4-R92	**α4-D102**	β2-P83	β2-A110
			α4-S87	α4-P93	α4-H109	β2-S84	
	+β2/−α4	(R)-SADU-3-72 (2)	α4-T108	β2-L58	**β2-D91**	β2-M101	β2-P122
			α4-H109	β2-Q60	β2-V92	β2-Y102	β2-P123
				β2-W62	β2-V93	**β2-E103**	β2-A124
				β2-K85	β2-L94	β2-V104	β2-I125
				β2-L89	β2-N97	β2-F106	β2-Y126
				β2-P90	β2-G100	β2-W120	β2-F148
		(R)-SADU-3-72 (3)	α4-R84	α4-H109	β2-K19	β2-I87	**β2-D91**
			α4-I85	α4-T111	β2-I21	β2-W88	**β2-E103**
			α4-P86	α4-K112	β2-L20	β2-L89	β2-F106
			α4-S87	α4-A113	β2-K85	β2-P90	β2-Y153
			α4-L89				

Residues in bold indicate hydrogen bond and/or a salt bridge formation (see Table 7 for more details).

Table 7
Hydrogen bond and salt bridge interactions for bupropion and SADU-3-72 isomers at luminal and non-luminal sites from the hα4β2 nAChR.

Domain	Site	Isomer (pose)	Hydrogen bond		Salt bridge
			Donor[a]	Acceptor[a]	Residues[a]
Luminal	L	(R)-BP (1)	LIG-M	β2-E239-S	β2-E239
		(R)-SADU-3-72 (1)	LIG-S	β2-E239-S	β2-E239 (1)[b]
			LIG-S	β2-T242-S	β2-E239 (2)[b]
		(S)-SADU-3-72 (1)	LIG-S	α4-E266-S	α4-E266
	Cyt	(R)-BP (1)	LIG-M	β2-E239-S	β2-E239 (1)[b]
					β2-E239 (2)[b]
		(R)-BP (2)	LIG-M	β2-E239-S	β2-E239 (1)[b]
					β2-E239 (2)[b]
		(R)-BP (3)	LIG-M	β2-E239-S	β2-E239 (1)[b]
					β2-E239 (2)[b]
		(S)-BP (1)	LIG-M	β2-E239-S	α4-E245
					β2-E239
		(R)-SADU-3-72 (1)	LIG-S	β2-E239-S	β2-E239
			LIG-S	α4-E245-S	α4-E245
		(R)-SADU-3-72 (2)	LIG-S	β2-E239-S	α4-E245
					β2-E239
		(S)-SADU-3-72 (1)	LIG-S	β2-E239-S	α4-E245
					β2-E239
		(S)-SADU-3-72 (2)	LIG-S	β2-E239-S	α4-E245
					β2-E239
		(S)-SADU-3-72 (3)	LIG-S	β2-E239-S	β2-E239
ECD-TMD	+α4/−β2	(R)-BP (1)	LIG-M	α4-D47-S	α4-D47
			LIG-M	α4-E266-S	
		(S)-SADU-3-72 (2)	LIG-S	α4-E50-S	α4-E50
			LIG-S	α4-D143-S	
	+β2/−α4	(R)-SADU-3-72 (1)	LIG-S	α4-E50-S	α4-E50
			LIG-S	α4-D47-S	α4-D47
	+β2/−β2	(S)-SADU-3-72 (1)	LIG-S	β2-D268-S	None
			LIG-S	β2-E47-S	
TMD	Intersubunit	(S)-SADU-3-72 (1)	LIG-S	α4-E266-S	α4-E266
			LIG-S	β2−D268-S	
	Intrasubunit	(S)-SADU-3-72 (2)	LIG-S	β2-D434-S	β2-D434
			LIG-S	β2-F231-M	β2-D236
ECD	Vestibular	β2			
		(S)-SADU-3-72 (1)	LIG-S	α4-D102-S	α4-D102
	Interfacial	+α4/−β2			
		(R)-SADU-3-72 (1)	LIG-S	β2-E103-S	β2-E103-S
		(S)-SADU-3-72 (2)	LIG-S	α4-D102-S	α4-D102
			LIG-S	α4-I95-M	
		+β2/−α4			
		(R)-SADU-3-72 (2)	LIG-S	β2-D91-S	β2-D91
			LIG-S	β2-E103-S	
			β2-K85-S	LIG-S	
		(R)-SADU-3-72 (3)	LIG-S	β2-E103-S	β2-D91
			LIG-S	β2-D91-S	

[a] M and S indicate whether the amino acid backbone or side chain atoms are involved in the H-bond.
[b] The number between parentheses indicates that more than one subunit of the same type is involved in the formation of the salt bridge.

(Arias et al., 2013b). A luminal binding site for both BP isomers was also found at the *Torpedo* (muscle-type) (i.e., between rings 6′ and 13′) (Arias et al., 2009) and hα7 (i.e., between ring 9′ and positon 10′) (Vázquez-Gómez et al., 2014) AChRs. The result indicating that only (S)-(+)-BP interacts with a site closer to the extracellular mouth of the hα7 AChR (i.e., between rings 13′ and 20′) suggests structural differences among AChRs. These structural differences, in turn, are reflected in the distinct pharmacological properties of (±)-BP among these AChR subtypes (Arias et al., 2009; Vázquez-Gómez et al., 2014).

Our docking results also show a cytoplasmic (Cyt) subsite for BP and SADU-3-72, near the cytoplasmic mouth of the ion channel. A similar result was found for (S)-(+)-mecamylamine interacting with the $(\alpha4)_2(\beta2)_3$ stoichiometry (Bondarenko et al., 2014). Interestingly, although BP and SADU-3-72 overlap both imipramine and mecamylamine sites, mecamylamine is confined to a site different to that for imipramine (Arias et al., 2010a). Finally, the Cyt subsite comprises the intermediate (−2′) and cytoplasmic (−5′) acidic rings, which are key structural components, especially the intermediate ring, in the process of cation permeation (Cymes and Grosman, 2012). In fact, salt bridges and H-bonds with residues at position -2′ were found for both BP and SADU-3-72.

In addition to the importance of the ion channel for the inhibitory activity of both SADU-3-72 and BP, the observed agreement between our molecular docking and previous photolabeling results reinforces the significance of the ECD-TMD junction in the interaction of SADU-3-72 with the hα4β2 AChR. Our docking results showed that (R)-SADU-3-72 interacts with α4-F217, whereas (R)-BP interacts with β2-F211. Interestingly, M1-Y213, the homologous residue at the *Torpedo* α1 subunit, was photolabeled by [^{125}I]SADU-3-72 preferably in the desensitized state in a (±)-BP-sensitive manner (Pandhare et al., 2012). The agreement between the molecular docking and photolabeling results might indicate that the hα4β2 AChR model used for our docking experiments is in the desensitized state. In fact, the evidence indicating that the interactive area for BP and SADU-3-72 is wider compared to that for other antidepressants (see previous paragraph), might reflect that our hα4β2 AChR model is in a different conformational state than

that in those studies. Since the m5-HT_{3A}R structure (i.e., 4PIR) used to construct the hα4β2 AChR model was in the bound state (i.e., potentially in the desensitized state) (Hassaine et al., 2014), it is possible that our model is in the desensitized state as well, supporting the observed differences.

Our results also support the importance of the ECD-TMD junction in the process of gating (reviewed in (Arias, 2010)). The most important structures for the gating process that correspond with the docking results for BP and SADU-7-32 are the β1-β2 loop, β8-β9 loop, Cys-loop, and β10-strand in the ECD, as well as the pre-M1 region and M2–M3 loop in the TMD. For example, (R)-SADU-3-72 forms a stable H-bond with α4-D143, which belongs to the Cys-loop typical of this receptor superfamily, as well as a H-bond and salt bridge with α4-E50 (β1-β2 loop), essential parts of the machinery involved in the process of normal gating (reviewed in (Arias, 2010)). Based on this observation, a simple allosteric mechanism can be devised for the inhibitory activity elicited by BP and SADU-7-32: these molecules may inhibit agonist-induced hα4β2 AChR function by structurally obstructing the process of gating, and consequently the opening of the ion channel, finally decreasing the passage of cations. In this regard, these compounds can be called negative allosteric modulators.

Molecular docking studies comparing the molecular interaction between BP and SADU-3-72 isomers showed that SADU-3-72, in addition to interacting with the same luminal sites as that for BP, it binds to several other sites located in the ECD and TMD where other compounds, but not BP, interact. Previous docking results support the importance of these domains. In particular, N,6-dimethyltricyclo[5.2.1.02,6]decan-2-amine enantiomers, noncompetitive antagonists of hα4β2 AChRs, interact with the TMD (Arias et al., 2013a) at the same intersubunit site found for (S)-SADU-3-72. The partial agonist varenicline binds to an allosteric site (called A2) in the ECD (Arias et al., 2015) corresponding to the interfacial +α4/−β2 site characterized for (S)-SADU-3-72 (pose 2). This evidence paves the way for additional inhibitory mechanisms, where partial agonists (as considered for varenicline (Arias et al., 2015)) or negative allosteric modulators may bind to this allosteric site producing conformational changes in the ECD that are translated into a decrease in ion channel activity.

This study gives information about the interaction of BP with α4β2 AChRs in different conformational states. More specifically, our results suggest that BP may inhibit α4β2 AChRs by allosteric mechanisms different to open channel blockade. In addition, this study paves the way for further photolabeling studies using (±)-SADU-3-72 to characterize the luminal site for (±)-BP in the resting state as well as the ECD-TMD junctional site in the desensitized state.

Acknowledgement

The authors thank the National Institute on Drug Abuse (NIDA) for the gift of bupropion.

Appendix A. Supplementary data

Supplementary data related to this article can be found at http://dx.doi.org/10.1016/j.neuint.2016.08.013.

References

Arias, H.R., 2009. Is the inhibition of nicotinic acetylcholine receptors by bupropion involved in its clinical actions? Int. J. Biochem. Cell Biol. 41, 2098–2108.
Arias, H.R., 2010. Positive and negative modulation of nicotinic receptors. Adv. Protein Chem. Struct. Biol. 80, 153–204 (R. Donev, Ed.), Elsevier Inc., USA.
Arias, H.R., Gumilar, F., Rosenberg, A., Targowska-Duda, K.M., Feuerbach, D., Jozwiak, K., Moaddel, R., Wainer, I.W., Bouzat, C., 2009. Interaction of bupropion with muscle-type nicotinic acetylcholine receptors in different conformational states. Biochemistry 48, 4506–4518.
Arias, H.R., Rosenberg, A., Targowska-Duda, K.M., Feuerbach, D., Jozwiak, K., Moaddel, R., Weiner, I.W., 2010. Tricyclic antidepressants and mecamylamine bind to different sites in the human α4β2 nicotinic receptor ion channel. Int. J. Biochem. Cell Biol. 42, 1007–1018.
Arias, H.R., Feuerbach, D., Targowska-Duda, K.M., Russell, M.M., Jozwiak, K., 2010. Interaction of serotonin selective reuptake inhibitors with neuronal nicotinic acetylcholine receptors in different conformational states. Biochemistry 49, 5734–5742.
Arias, H.R., Feuerbach, D., Targowska-Duda, K.M., Aggarwal, S., Lapinsky, D.J., Jozwiak, K., 2012. Structural and functional interaction of (±)-2-(*N-tert*-butylamino)-3'-iodo-4'-azidopropiophenone, a photoreactive bupropion derivative, with nicotinic acetylcholine receptors. Neurochem. Int. 61, 1433–1441.
Arias, H.R., Targowska-Duda, K.M., Jozwiak, K., 2013. N,6-dimethyltricyclo [5.2.1.02,6]decan-2-amine enantiomers interact with the human α4β2 nicotinic acetylcholine receptor at luminal and non-luminal domains. OA Biochem. 1, 11.
Arias, H.R., Fedorov, N.B., Benson, L.C., Lippiello, P., Gatto, G.J., Feuerbach, D., Ortells, M.O., 2013. Functional and structural interaction of (-)-reboxetine with the human α4β2 nicotinic acetylcholine receptor. J. Pharmacol. Exp. Ther. 344, 113–123.
Arias, H.R., Biała, G., Kruk-Słomka, M., Targowska-Duda, K.M., 2014. Interaction of nicotinic receptors with bupropion: structural, functional, and pre-clinical perspectives. Recept. Clin. Investig. 1, 30–45.
Arias, H.R., Feuerbach, D., Targowska-Duda, K.M., Kaczor, A.A., Poso, A., Jozwiak, K., 2015. Pharmacological and molecular studies on the interaction of varenicline with different nicotinic acetylcholine receptors. Potential mechanism underlying partial agonism at human α4β2 and α3β4 subtypes. Biochem. Byophys. Acta - Biomembr. 1848, 731–741.
Arias, H.R., 2006. Ligand-gated ion channel receptor superfamilies. In: Arias, H.R. (Ed.), Biological and Biophysical Aspects of Ligand-gated Ion Channel Receptor Superfamilies. Research Signpost, Kerala, India, pp. 1–25.
Baker, N.A., Sept, D., Joseph, S., Holst, M.J., McCammon, J.A., 2001. Electrostatics of nanosystems: application to microtubules and the ribosome. Proc. Natl. Acad. Sci. U. S. A. 98, 10037–10041.
Bondarenko, V., Targowska-Duda, K.M., Jozwiak, K., Tang, P., Arias, H.R., 2014. Molecular interactions between mecamylamine enantiomers and the transmembrane domain of the human α4β2 nicotinic neceptor. Biochemistry 53, 908–918.
Brooks, B.R., Bruccoleri, R.E., Olafson, B.D., States, D.J., Swaminathan, S., Karplus, M., 1983. Charmm: a program for macromolecular energy, minimization, and dynamics calculations. J. Comput. Chem. 4, 187–217.
Cheng, Y., Prusoff, W.H., 1973. Relationship between the inhibition constant (K_i) and the concentration of inhibitor which causes 50 percent inhibition (IC_{50}) of an enzymatic reaction. Biochem. Pharmacol. 22, 3099–3108.
Cymes, G.D., Grosman, C., 2012. The unanticipated complexity of the selectivity-filter glutamates of nicotinic receptors. Nat. Chem. Biol. 8, 975–981.
Grubmueller, H., 1996. SOLVATE V. 1.0, Theoretical Biophysics Group. Institute for Medical Optics, Ludwig-Maximilians University, Munich.
Hassaine, G., Deluz, C., Grasso, L., Wyss, R., Tol, M., Hovius, R., Graff, A., Stahlberg, H., Desmyter, A., Moreau, C., Li, X.D., Poitevin, F., Vogel, H., Nury, H., 2014. X-ray structure of the mouse serotonin 5-HT3 receptor. Nature 512, 276–281.
Hsyu, P.H., Singh, A., Giargiari, T.D., Dunn, J.A., Ascher, J.A., Johnston, J.A., 1997. Pharmacokinetics of bupropion and its metabolites in cigarette smokers versus nonsmokers. J. Clin. Pharmacol. 37, 737–743.
Kamens, H.M., Stephens, S.H., Ehringer, M.A., 2011. Human genetic studies of CHRN genes. In: Arias, H.R. (Ed.), Pharmacology of Nicotinic Acetylcholine Receptors from the Basic and Therapeutic Perspectives. Research Signpost, Kerala, India, pp. 19–43.
Lapinsky, D.J., Aggarwal, S., Nolan, T.L., Surratt, C.K., Lever, J.R., Acharya, R., Vaughan, R.A., Pandhare, A., Blanton, M.P., 2012. (±)-2-(*N-tert*-Butylamino)-3'-[^{125}I]-iodo-4'-azidopropiophenone: a dopamine transporter and nicotinic acetylcholine receptor photoaffinity ligand based on bupropion (Wellbutrin, Zyban). Bioorg. Med. Chem. Lett. 22, 523–526.
Lewards, E.G., 2011. Computational Chemistry. Introduction to the Theory and Applications of Molecular and Quantum Mechanics, second ed. Springer, New York.
Mathur, A., Shankaracharya Vidyarthi, A.S., 2011. SWIFT MODELLER: a JAVA based GUI for molecular modeling. J. Mol. Model. 17, 2601–2607.
Moore, M.A., McCarthy, M.P., 1995. Snake venom toxins, unlike smaller antagonists, appear to stabilize a resting state conformation of the nicotinic acetylcholine receptor. Biochim. Biophys. Acta 1235, 336–342.
Pandhare, A., Hamouda, A.K., Duddempudi, B.S.P.K., Lever, J.R., Lapinsky, D.J., Jansen, M., Cohen, J.B., Blanton, M.P., 2012. Bupropion binds to two sites in the *Torpedo* nicotinic acetylcholine receptor transmembrane domain: a photoaffinity labeling study with the bupropion analogue [^{125}I]-SADU-3-72. Biochemistry 51, 2425–2435.
Papke, R.L., Trocmé-Thibierge, C., Guendisch, D., Al Rubaiy, S.A.A., 2011. S.A. Bloom Electrophysiological perspectives on the therapeutic use of nicotinic acetylcholine receptor partial agonists. J. Pharmacol. Exp. Ther. 337, 1–13.
Pedretti, A., Villa, L., Vistoli, G., 2004. VEGA - an open platform to develop chemo-bio-informatics applications, using plug-in architecture and script programming. J. Comput. Aided. Mol. Des. 18, 167–173.
Phillips, J.C., Braun, R., Wang, W., Gumbart, J., Tajkhorshid, E., Villa, E., Chipot, C.,

Skeel, R.D., Kale, L., Schulten, K., 2005. Scalable molecular dynamics with NAMD. J. Comput. Chem. 26, 1781–1802.
Šali, A., Blundell, T.L., 1993. Comparative protein modelling by satisfaction of spatial restraints. J. Mol. Biol. 234, 779–815.
Thompson, J.D., Higgins, D.G., Gibson, T.J., 1994. CLUSTAL W: improving the sensitivity of progressive multiple sequence Alignment through sequence weighting, position-specific gap penalties and weight matrix choice. Nucleic Acids Res. 22, 4673–4680.
Trott, O., Olson, A.J., 2010. AutoDock Vina: improving the speed and accuracy of docking with a new scoring function, efficient optimization and multithreading. J. Comput. Chem. 31, 455–461.
Vázquez-Gómez, E., Arias, H.R., Feuerbach, D., Miranda-Morales, M., Mihailescu, S., Targowska-Duda, K.M., Jozwiak, K., García-Colunga, J., 2014. Bupropion-induced inhibition of α7 nicotinic acetylcholine receptors expressed in heterologous cells and neurons from dorsal raphe nucleus and hippocampus. Eur. J. Pharmacol. 740, 103–111.